Rossby Adjustment over a Slope in a Homogeneous Fluid

S. E. ALLEN

Department of Oceanography, University of British Columbia, Vancouver, British Columbia, Canada

(Manuscript received 17 September 1993, in final form 27 February 1996)

ABSTRACT

The adjustment of ocean currents initially traveling over a topographic change in depth has previously been investigated in the limit of a discontinuous depth change. The present work is an extension to a linear, continuous depth change. Differences in the time-dependent flow are shown to follow from the different properties of double Kelvin waves over steps and slopes. Over a slope, double Kelvin waves have a series of cross-slope modes and can have group speeds in both directions along the slope. Thus, energy propagates both ways along the slope.

The steady state over a linear slope is argued to be similar to that for a step escarpment. The slope separates the streamlines, isolating the flow on the two sides of the slope. The results of a series of numerical experiments are given in order to describe the transient flow and to examine the effect of varying the two governing parameters: the nondimensional gradient of the slope and the nondimensional slope width. The slope gradient is found to define the timescale of formation of the tongue and the slope width to define the cross-sectional shape.

1. Introduction

Topography, through topographic steering, strongly guides the slow motions of the oceans. Willmott (1984) investigated the forced double Kelvin waves generated over a topographic step in order to explain cold water streamers emanating from Cape Mendocino and lying over the Mendocino escarpment. The step geometry is convenient to work with analytically and has been extensively investigated: Johnson (1985), Gill et al. (1986), Johnson (1990), Johnson and Davey (1990), and Spitz and Nof (1991) among others. Extension to continuous escarpments is more recent; Willmott and Grimshaw (1991) considered source–sink flow over a wedge-shaped escarpment that is discontinuous at the coast, and Johnson (1993) considered scattering of a low-frequency Kelvin wave over continuous topography. The topography in the ocean is continuous, if very steep in places, and so the problem of the adjustment of flow over a continuous, linear slope is considered here in order to generalize the results that have been obtained over step topographies. In particular, as we shall use an initial surface discontinuity to force the flow, the present work can be viewed as a generalization of Gill et al. (1986).

To show the strong similarities between flow over a step and a slope, we will consider the linear limit of weak flows and find the form of the steady state. The differences between a step and slope are in the time-dependent response and are illustrated through use of a numerical model.

Linear flows are tractable through wave theory and the properties of the waves in the problem are critical to the solution. An escarpment (a topographic step or slope) acts as a waveguide for double Kelvin waves (Rhines 1967). The dispersion relation and wave shape for these subinertial waves were derived by Longuet-Higgins (1968a,b) over a step and over a finite slope. Over a flat bottom, in an infinite domain where the rotation is uniform, no propagating subinertial frequency waves can exist. The superinertial oscillations consist of Poincaré waves. Thus, if the motion produced by Rossby adjustment over a slope is considered as a combination of waves, the two types of waves, Poincaré and double Kelvin, will coexist in different frequency bands.

The dispersion curve for double Kelvin waves is similar to that for Rossby waves in that the waves have phase velocity in one direction only, the direction which keeps the shallow water on the right in the Northern Hemisphere. The long waves have group velocities, c_g, in the same direction as the phase velocity, c_p, and in the limit of the alongslope wavenumber, $m \to 0$, the long waves are nondispersive. For a linear slope, the mode 0 waves have group and phase speeds bounded by

$$c_g = c_p \geqslant \sigma\sqrt{gh} = \left(\frac{R\Delta h}{hW}\right)\sqrt{gh}$$

and by

Corresponding author address: Dr. Susan E. Allen, Department of Oceanography, University of British Columbia, 6270 University Blvd., Vancouver, BC V6T 1Z4, Canada.
E-mail: allen@ocgy.ubc.ca

$$c_g = c_p \geq \left(\frac{\Delta h^{1/2}}{h}\right)\sqrt{gh},$$

where h is the depth of the deep water, $R = (gh)^{1/2}/f$ is the Rossby radius, W is the width of the slope, Δh is the depth change across the slope, and $\Delta h^{1/2}$ is the difference across the slope of the square root of the depth. The short waves have group velocity in the opposite direction to the phase velocity. For $W/R = 5$ and $\Delta h = 0.5h$, at wavenumber $q \approx 1.3/R$, the group velocity for mode 0 is zero. Wave cross sections across the slope show that, at the longest wavelengths, the wave energy is spread across most of the slope, whereas the energy at the shorter wavelengths is concentrated at the top of the slope.

The forcing is taken to be small enough that the nonlinear advection terms can be considered negligible. The effects of finite flow are discussed in Allen (1988).

In section 2 the problem is defined, the initial adjustment and steady state described, and the energy propagation estimated. In sections 3 and 4 the results of the linear numerical code are described. The results from the numerical simulations are discussed in terms of the parameters that affect the flow: the nondimensional width of the slope, W/R, and the nondimensional slope gradient, σ, which is an upper bound on the nondimensional long wave speed along the slope.

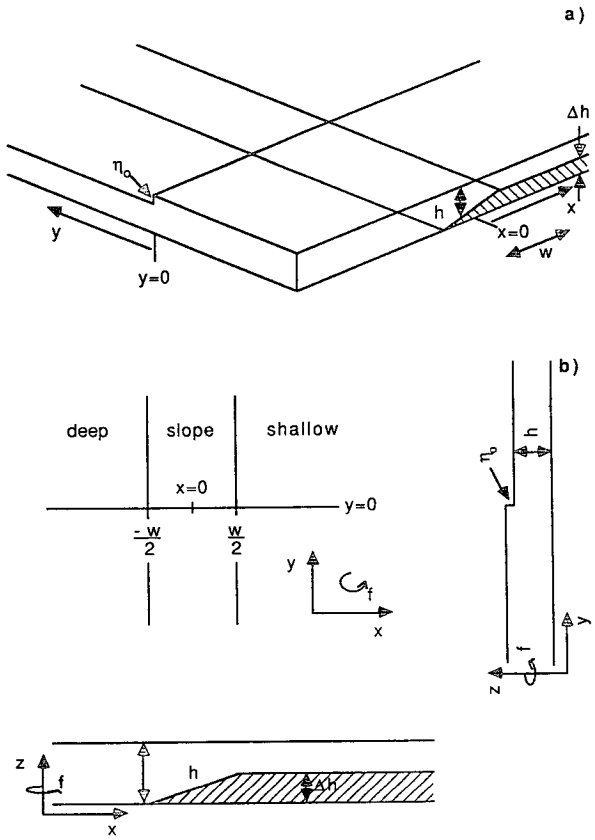

FIG. 1. The initial configuration showing (a) a perspective view and (b) a plan view with cross sections.

2. Governing equations

The governing equations are the linear shallow water equations,

$$\frac{\partial u}{\partial t} - fv = -g\frac{\partial \eta}{\partial x} \tag{1a}$$

$$\frac{\partial v}{\partial t} + fu = -g\frac{\partial \eta}{\partial y} \tag{1b}$$

$$\frac{\partial \eta}{\partial t} + \frac{\partial}{\partial x}(hu) + \frac{\partial}{\partial y}(hv) = 0, \tag{1c}$$

where η is the surface elevation and $[u(x, y, t), v(x, y, t)]$ is the horizontal velocity of the fluid. Let the x axis lie along the discontinuity in surface height and let the y axis lie along the center of the slope, as shown in Fig. 1. The initial surface height is

$$\eta = \eta_I = \begin{cases} \eta_0, & y < 0 \\ 0, & y > 0, \end{cases} \tag{2}$$

where η_0 can be considered positive without loss of generality. The depth of the fluid is h_a for $x < -W/2$, h_b for $x > W/2$, and varies linearly between these two regions.

In order to obtain the steady-state solution, time derivatives in (1) are set to zero. Cross-multiplying the momentum equations gives $\partial u/\partial x + \partial v/\partial y = 0$, which implies that geostrophic flow has zero divergence. Substituting into the conservation of mass equation gives $u\partial h/\partial x + v\partial h/\partial y = 0$. This result is the familiar tendency of steady geostrophic flow to follow the contours of depth. In the configuration considered here, the topography is independent of y. Thus, over the slope, $u = 0$ and from (1b), $\partial \eta/\partial y = 0$. The value of η or v completes the solution over the slope and is given in section 2b.

The steady-state equation over the flat regions is the conservation of potential vorticity equation derived from (1):

$$R^2\nabla_h^2\eta - \eta = -\eta_I, \tag{3}$$

where $\nabla_h^2 = \partial^2/\partial x^2 + \partial^2/\partial y^2$. Over the flat-bottomed basins far from the slope the flow will tend to be independent of x, and the steady-state flow will tend to the solution over a flat bottom as given in Gill (1982). The solution in the vicinity of the slope is given by (3) with boundary conditions that the solution must tend to the solution over a flat bottom away from the slope (Gill 1982) and that it must match the solution over the slope at the slope edges. The solution is similar to the solutions of Gill et al. (1986) and is illustrated in Fig. 3.

The flat-bottom solution far from the slope implies a flux in the jet of

$$\int_{-\infty}^{\infty} dy\, hu = \eta_0 f R^2 = \frac{\eta_0 g h}{f}, \qquad (4)$$

(Gill 1982). Thus, the flux is proportional to the local depth of the fluid. Since the depths on the two sides of the slope are unequal, the fluxes do not match at the slope. The difference in the flux into and out of the slope region is

$$\eta_0 f [R_a^2 - R_b^2] = \frac{\eta_0 g}{f} [h_a - h_b], \qquad (5)$$

where $R_a = (gh_a)^{1/2}/f$ and $R_b = (gh_b)^{1/2}/f$ are the Rossby deformation radii on either side of the slope. The difference, (5), gives the rate at which fluid must accumulate or be removed from the slope region.

a. Early stages of adjustment

The earliest stages of adjustment are determined by the radiation of Poincaré waves since these waves, being superinertial, have timescales smaller than the subinertial, double Kelvin waves. Thus, on the order of an inertial period the flow is, approximately, that given by the solution over a flat bottom based on the local depth. For η_0 positive, consider $h_a > h_b$ so that the jet flows from the deep water to the shallow water. There is a net flux into the slope region that results in an accumulation of fluid in the vicinity of the slope. By conservation of potential vorticity, the change in vorticity, ζ, is given by

$$h \frac{\partial \zeta}{\partial t} = f\left(\frac{\partial \eta}{\partial t} + u \frac{\partial h}{\partial x}\right) = -f\left(\frac{\partial u}{\partial x} + \frac{\partial v}{\partial y}\right) \qquad (6)$$

and the latter relation is arrived at by substitution of (1c).

If we consider the flow after it has undergone Rossby adjustment given by the local depth in the two flat regions, the velocity along the line $y = 0$ is

$$u = \frac{1}{2} \eta_0 \left(\frac{g}{h}\right)^{1/2}, \quad v \approx 0 \qquad (7)$$

away from the slope. Integrating (6) across the slope region at $y = 0$ gives the average $h\zeta$ as proportional to the difference in u between the two edges of the region. From (7) for flow up the slope with $dh/dx < 0$, anticyclonic vorticity is produced over the slope.

Therefore, the flow has the same properties as flow over a step. If the flow is upslope, anticyclonic vorticity will be generated. As illustrated in Fig. 2, this anticyclonic vorticity, when added to the jet, bends the jet in such a way that it moves around a "tonguelike" accumulation of fluid. It can be shown that for flow downslope, cyclonic vorticity is generated. Thus, the tongue is always formed keeping the shallow water to the right in the Northern Hemisphere as is the case for flow over a step. The dispersion relation for double Kelvin waves, which carry information along the slope, implies that the long waves have group velocity in the direction the tongue tends to form but the short waves have group velocity in the opposite direction (Longuet-Higgins 1968b).

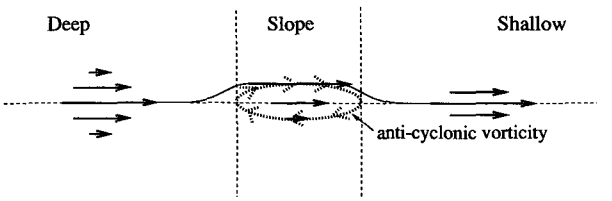

FIG. 2. Plan view of a schematic of the response of the current to the slope. Generation of anticyclonic vorticity at the slope strengthens the flow on one side of the jet and weakens it on the other. The position at which the jet crosses the slope moves continually away from the original discontinuity, keeping the shallow water on the right.

b. Steady state

To determine the details of the steady state, that is, the value of the surface height or the velocity v over the slope, the time evolution of the flow must be considered. As the governing equations are linear, the principle of superposition holds and any flow can be considered as the sum of the steady state and the waves generated by the initial conditions or formally as the Fourier superposition:

$$\eta = \eta_{ss} + \int_0^{\infty} d\omega \int_{-\infty}^{\infty} dm[\eta_c(\omega, m, x) \cos(my - \omega t) + \eta_s(\omega, m, x) \sin(my - \omega t)], \qquad (8)$$

where each η_c and each η_s satisfies the ordinary differential equation, derived from (1),

$$\left[g \frac{\partial}{\partial x}\left(h \frac{\partial}{\partial x}\right) + (\omega^2 - f^2) - ghm^2 - \frac{gmf}{\omega} \frac{\partial h}{\partial x}\right] \eta = 0 \qquad (9)$$

and where the solution for $\omega = 0$ is termed η_{ss}.

For a similar problem, Willmott and Grimshaw (1991) derived analytically the steady-state solution over a wedge-shaped escarpment. They considered a source–sink geometry with a rigid lid so that Poincaré waves were excluded. As time $t \to \infty$, the only contribution to the Fourier integral was due to a pole at $m = 0$ in η_s. Johnson and Davey (1990) found a similar result over a vertical step including a free surface. This pole corresponds to the long double Kelvin wave.

Consider the Rossby adjustment problem: the surface elevation is initially a step function (in y) but the final steady state, over the slope, is constant in y. Step function implies the presence of a pole at $m = 0$ in η_s. Analogous to the problem solved in Willmott

and Grimshaw (1991), it can be argued that this pole should determine the steady-state solution and that it corresponds to long double Kelvin waves.

Longuet-Higgins (1968b) gives the dispersion relation and governing equation for double Kelvin waves over a slope. All long waves ($m \to 0$) have group velocities that keep the shallow water to the right. Furthermore, for low-frequency waves the equation and boundary conditions governing the cross-slope mode shape are of Sturm–Liouville form, and thus the modes form a complete set (over the slope itself). Hence, the slope acts as a waveguide; these long waves determine the steady state and, because they travel in only one direction along the slope, the solution is asymmetric.

For the case $h_a > h_b$ for which the long waves travel from negative y to positive y, the waves carry the surface height information from $y \to -\infty$. The surface height for y negative initially is a constant η_0, and as the long waves travel toward positive y and as they form a complete set, the final surface height over the slope is this constant. For the case $h_b > h_a$, a similar argument gives $\eta = 0$ over the slope.

The surface height over the slope is constant and there is no flow over the slope in the steady state. The fluid over the slope is *stagnant* and completely separates the flow in the deep basin from that in the shallow basin. Figure 3 shows a wire-mesh plot of the surface elevation of the steady-state solution. The potential vorticity of the steady-state solution, $Q = \zeta h - f\eta$, in the region over the slope in the direction the long double Kelvin waves travel, is less than that of the initial state by $f\eta_0$. It is unchanged in all other regions.

The steady-state solution for the slope is thus very similar to solution for a step found by Gill et al. (1986) with the surface height over the slope a constant and equal to that over a step.

c. *Presence of a coast*

Now consider the case of a vertical coast parallel to the original discontinuity in the direction in which the short waves propagate. The surface elevation at the coast will be maintained by Kelvin waves to be the surface elevation from the deep water. As shown above, long double Kelvin waves will carry this surface height information away from the wall. The steady-state surface elevation over the slope will be a constant and will completely separate the flow in the deep basin from that in the shallow basin.

d. *Energy propagation*

It is perhaps not surprising that the steady solution for the slope is very similar to the steady state for the step in that the steady state is determined by the very longest waves, and for these the slope appears steplike. However, energy transport depends on the full spectrum of waves and is not the same for a step and a slope. The step only supports group speeds in one direction, whereas short waves on the slope travel in the opposite direction.

The energy available to the double Kelvin waves can be conceptually separated into two parts: the energy available from the initial surface discontinuity over the slope and the energy from the incoming jet. The energy from the jet increases with time and feeds the surface height change, which moves in the positive direction along the slope. This energy is further discussed in section 3c. In this section we will consider the energy available from the initial surface discontinuity over the slope as a portion of it moves in the negative direction.

For simplicity we will only consider the case $h_a > h_b$, that is, the water is deep, denoted by subscript D, for $x < -W/2$ and shallow, denoted by subscript S, for $x > W/2$.

Multiplying (8) by $\sin(my)$ and then integrating over all y gives η_s as the Fourier sine transform of the initial surface height minus the steady state:

$$-\frac{\eta_0}{2\pi}\begin{cases}\dfrac{m}{m^2+\alpha_D^2}+\left(\dfrac{m}{m^2+\alpha_D^2}-\dfrac{1}{m}\right)\\ \times\exp[(x+W/2)(\alpha_D^2+m^2)^{1/2}], \quad x<-W/2\\ \dfrac{-1}{m}, \quad |x|<W/2\\ \dfrac{m}{m^2+\alpha_S^2}+\left(\dfrac{m}{m^2+\alpha_S^2}-\dfrac{1}{m}\right)\\ \times\exp[-(x-W/2)(\alpha_S^2+m^2)^{1/2}], \quad x>W/2.\end{cases} \tag{10}$$

In order to estimate the energy traveling in the negative direction along the slope (that is, in the opposite direction of the long double Kelvin waves) it is necessary to estimate the separation between the Poincaré and double Kelvin waves. Assuming that the Poincaré waves are generated in the same way as if the bottom was locally flat, the part of the sine transform (10) attributable to the Poincaré waves is $m/(m^2 + \alpha_l^2)$, where α_l is the reciprocal of the local Rossby radius. This assumption is justified by the numerical experiments; see Fig. 4. Making the geostrophic approximation we can approximate the velocity: $u \approx (m/\alpha_l)(\eta Rf/h)$ and $v \approx [(m + \alpha_l)/\alpha_l](\eta Rf/h)$. Then we integrate over wavenumber from m_{cn} to infinity, where m_{cn} is the wavenumber corresponding to zero group speed. To estimate an upper bound, m_{cn} was approximated as m_{c0}, the critical wavenumber for the gravest mode. Evaluation gives the energy at any x on the slope as

$$\frac{1}{\pi^2}\, g\eta_0^2 h\left(-\frac{\alpha_l}{2(\alpha_l^2+m_c^2)}-\frac{1}{2\alpha_l}\ln\frac{m_c^2}{\alpha_l^2+m_c^2}+\frac{1}{m_c}-\frac{\pi}{2\alpha_l}+\frac{1}{\alpha_l}\arctan\frac{m_c}{\alpha_l}\right), \tag{11}$$

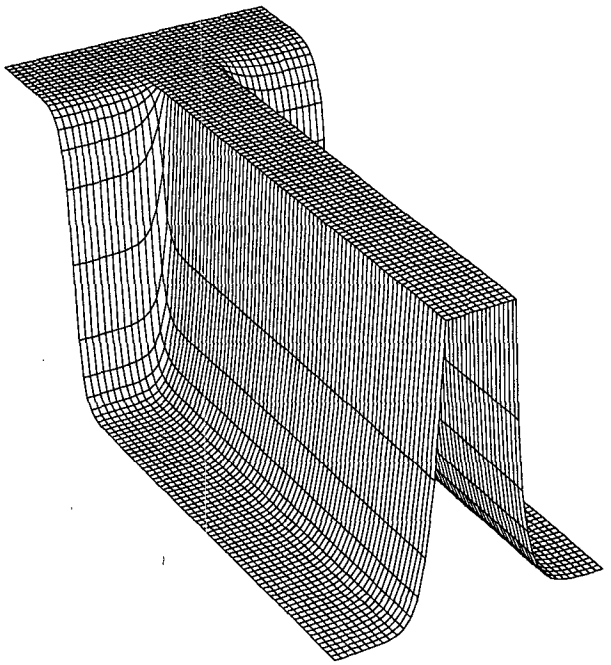

FIG. 3. A wire mesh showing the surface elevation of the steady-state solution. The x axis runs from top right to lower left. The slope lies under the "tongue" protruding toward the lower right; the shallow water is towards the lower left. Grid lines are $R_D/2$ apart. The slope has width $5.0R_D$ and the depth change is 50%.

where h is the local depth. The total energy originally over the slope available to double Kelvin waves is $0.125 g\eta_0^2 h/\alpha_l$. For the case of a slope five Rossby radii wide and with a depth change of 50%, $m_{c0} = 1.32$, giving an upper bound on the energy traveling in the negative direction, integrated across the width of the slope, of 20%. The amount of energy traveling in the negative direction increases as m_c decreases and thus increases for increasing slope width or decreasing slope gradient.

Energy traveling in both directions along the slope is dependent on the finite width of the slope and is not observed over step topography.

3. Results from the numerical code

This section presents the results produced by the linear numerical simulation. The numerical code is a modified version of the one used to simulate flow over a step and is described in Gill et al. (1986). The domain of the numerical simulation is rectangular and scaled in terms of the deep water Rossby radius, R_D. The maximum (and usual) grid size is $R_D/2$. The depth varies in the x direction and the boundary conditions are periodic or radiative/sponge in x and periodic or free-slip in y. The flow is forced by adding fluid to the region on one side of the forcing discontinuity. Rather than adding all the fluid at $t = 0$, the fluid addition is spread over 5 inertial periods to reduce the amplitude of the Poincaré waves produced. There is no explicit viscosity in the model.

a. Description of the observed flow

First, a detailed, principally qualitative, description of the flow is presented for a particular set of parameters: a slope from deep water to shallow with a slope width of five Rossby radii and a depth change of 50%; that is, $W/R = 5.0$ and $\sigma = 0.1$.

Within the first inertial period, an initial adjustment to the local depth is reached. The surface contours at this time are shown in Fig. 4. Over the flat basins away from the influence of the slopes the steady-state solution in the absence of topography is realized. Over the slope, the jet varies in width depending on the depth of the fluid, being wider in the deeper water (it scales, as expected, with the Rossby radius). These results verify the assumption made in section 2 that the fluid adjusts over a short timescale to a solution close to the steady state over a flat bottom based on the local depth.

Fluid accumulates over the slope as the jet flows from deep water into the shallow water. The jet deflects to the right (looking downstream) turning out along the slope, crossing the slope, flowing back along the slope and turning to join the jet over the shallow basin. As time increases, the peak height increases above η_0 and the peak widens to approximately 4/5 the width of the slope. The peak advances with the tongue and decreases again in width as the tongue narrows. Behind the peak a trough forms (after 10 inertial periods) and behind that a second peak forms (after 20 inertial periods). After 50 inertial periods, dispersion of wavenumbers and modes leads to the dramatic structure of the tongue shown in Fig. 5. The leading long wave,

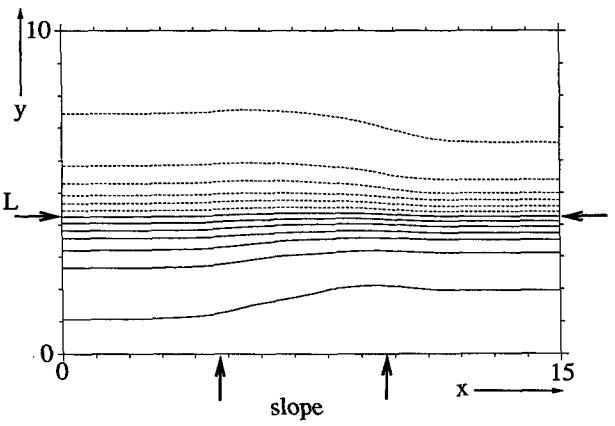

FIG. 4. Results of the simulation for $W/R = 5.0$ and $\Delta h = 0.5/hD$. The surface height contours are shown after 1 inertial period. Distance is in units of R_D; L marks the position of the initial discontinuity and the arrows along the x axis mark the bottom and top of the slope, respectively. The solid contours are $\eta \leq \eta_0/2$ and the dotted ones are $\eta < \eta_0/2$. The walls are well below and above the region shown.

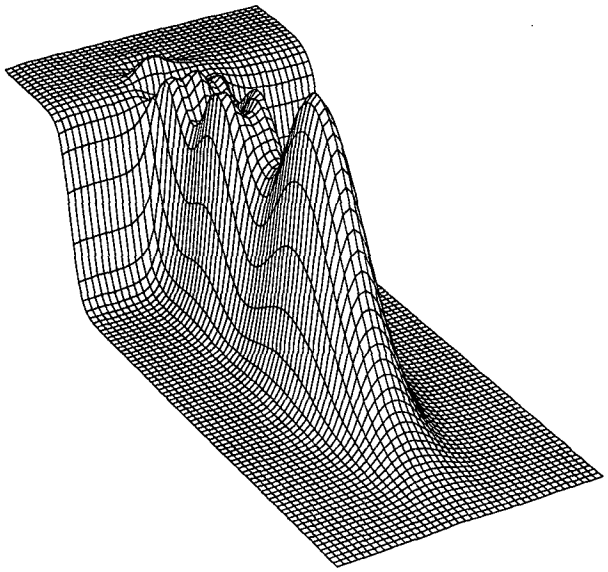

FIG. 5. Results for the same simulation as Fig. 4. A surface height wire mesh is shown after 50 inertial periods. Alignment as for Fig. 3.

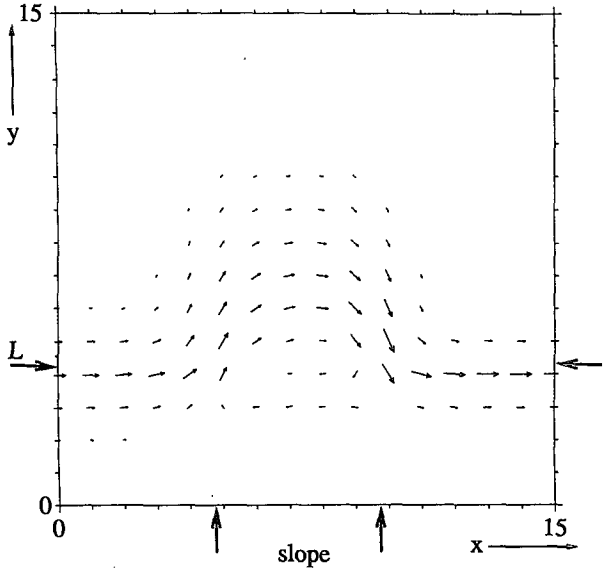

FIG. 6. Results for the same simulation as Fig. 4. The velocity field is shown after 10 inertial periods.

gravest mode (mode 0) is visible followed by mode 2 and then mode 4 long waves. As each wave mode passes, the surface elevation over the ridge comes closer to being independent of x and equal to η_0. Traveling in the other direction along the slope, the short gravest-mode waves are visible.

The flow field after 10 inertial periods is shown in Fig. 6. The streamlines nearly follow the surface contours, as they would if the flow was steady. Most of the flow over the slope is around the front of the accumulated fluid. However, there is a weak back flow downslope behind the peak, giving closed anticyclonic streamlines over the slope.

A slope from shallow water to deep water is essentially the mirror image of the above about the line of the initial discontinuity and with the surface height inverted. The tongue travels in the opposite direction, still with the shallow water to its right and carries a negative change in surface height.

b. *Presence of a coast*

If the surface discontinuity is moved close to a coast modeled as a free-slip wall in such a way that the tongue propagates away from the wall, the pattern of the tongue produced is qualitatively the same as in the absence of the wall. The height of the depth change is reduced to be equal to the depth at the wall in the deep water. In order to resolve the flow near the wall, the grid size must be reduced. For a grid size of $R_D/8$ the surface height at the wall is constant within 2% after 100 inertial periods.

c. *Energy of the flow*

The kinetic energy in the simulation domain is plotted versus time in Fig. 7. The initial adjustment to local geostrophic flow can be seen and is essentially complete by the sixth inertial period, one period after the

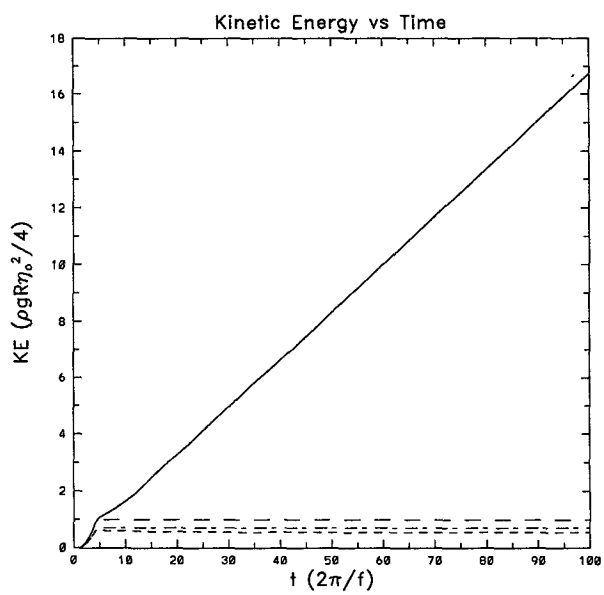

FIG. 7. Graph of the kinetic energy per unit length along the x axis. Same parameters as Fig. 4. Time is in inertial periods. Note that the forcing is spread over 5 inertial periods; see the text. Solid: over slope, $x > 0$; long dashed: away from the slope, deep water; long-short dashed: away from the slope, shallow water; short dashed: over slope, $x < 0$.

forcing is stopped. There is a slight "overshoot" in the kinetic energy, which is due to the large v velocity components necessary to relax the forcing discontinuity. After this first rise in kinetic energy, there is a slow rise as the tongue grows and the jets on each side of it become longer. This rise indicates that the bottom topography allows more kinetic energy to be released from the spatial variation in the surface height than is possible in the absence of topography.

The energy continues to increase as potential energy is converted to kinetic energy. From where the energy appears to come depends on the choice of origin for the calculation of the potential energy. Taking the obvious choice of the undisturbed fluid height, the incoming jet energy is higher than the outgoing and this is the source of energy for $h_a > h_b$, that is, an elevated tongue. If $h_a < h_b$, the flux difference between the jets is overshadowed by the potential energy release of the tongue formation, as the tongue is a depression.

However, if we take the symmetric choice, the midpoint of the two original elevations, $\eta_0/2$ as the origin for the potential energy calculation, then there is no energy flux in either jet. The steady-state tongue cross section has less potential energy than the undisturbed fluid and this is the source of the kinetic energy (as in the depression case above).

4. Effect of varying the parameters

a. *Effect of* σ

Varying the slope gradient, $\sigma = (h_b - h_a)R_D/(Wh_D)$, primarily effects the timescale of the adjustment. The most obvious instance of this effect is in the speed of propagation of the disturbance along the slope. In the positive direction along the slope, that is, the direction in which the long double Kelvin waves move, the leading edge of the disturbance is easily characterized by the foremost position over the slope where the surface elevation is $\eta_0/2$. After 5 inertial periods the variation of this position with time is observed to be approximately linear. The propagation speed of the disturbance is determined by a least squares fit on position versus time data from the 15th to the 100th inertial period and is plotted for various values of σ in Fig. 8. As expected, the values are within 1% of the group speed of the long mode-0 double Kelvin wave.

In the negative direction along the slope, the leading edge of the disturbance is defined to be the furthest point, from the line of the forcing discontinuity, where the velocity $|\vec{u}| = \sqrt{u^2 + v^2} \leq \epsilon u_{\max}$. The velocity, $u_{\max}$, is the maximum velocity observed in Rossby adjustment over a flat bottom of the same depth as the deep water. The parameter ϵ is taken to be 0.005. One run ($W/R = 5.0$, $\Delta h = 0.5h_D$) was repeated for $\epsilon = 0.0075$ and yielded results differing by less than 1%. The speed of propagation alongslope is determined by a least squares fit to the data between the 15th and the 100th inertial period and is plotted in Fig. 8.

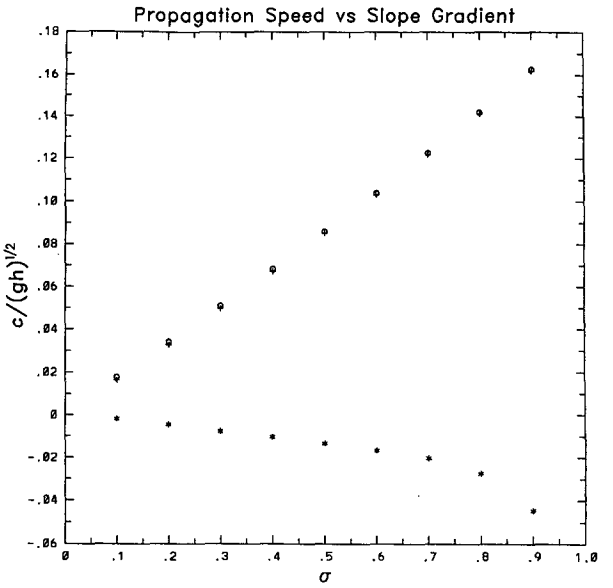

FIG. 8. Plot of the propagation speed of the tongue, c, nondimensionalized by $\sqrt{gh}$ versus σ. Plus sign: $x > 0$, using surface height method; open circle: $x > 0$, using velocity method; asterisk: $x < 0$, using velocity method; see text.

The forward propagation speed can also be calculated using the velocity. This method gives values up to 10% higher than the surface elevation method.

b. *Effect of* W/R

In Fig. 9, the surface height contours after 30 inertial periods are plotted, for a slope of width $W = 0.5R$ and for a slope of width $W = 7.5R$ (both having $\sigma = 0.1$). The speed of propagation is slightly greater for the wider slope. However, the main difference is the shape of the disturbance. For small slope widths, $W < 1.0R$, the disturbance is symmetrical as was observed by Johnson and Davey (1990) over a step; see their Fig. 3. For larger slope widths the disturbance is not symmetric; the peak first forms approximately $1R$ from the top of the slope. Thus, the wider the slope the more asymmetric the pattern. As the disturbance propagates, the leading portion becomes more symmetric, whereas the portion near the initial discontinuity remains asymmetric as can be seen in Fig. 5, which shows the surface contours after 50 inertial periods for a slope of $W/R = 5$.

The asymmetry is easily understood in terms of double Kelvin waves. The higher the wavenumber and the wider the slope, the more the waveform is concentrated at the top of the slope. The long waves move faster, leaving the short waves behind. The long waves are nearly symmetric for all slope widths whereas the short waves, which form the peak, are asymmetric, particularly for wide slopes. The rate of formation of the peak decreases as slope width increases.

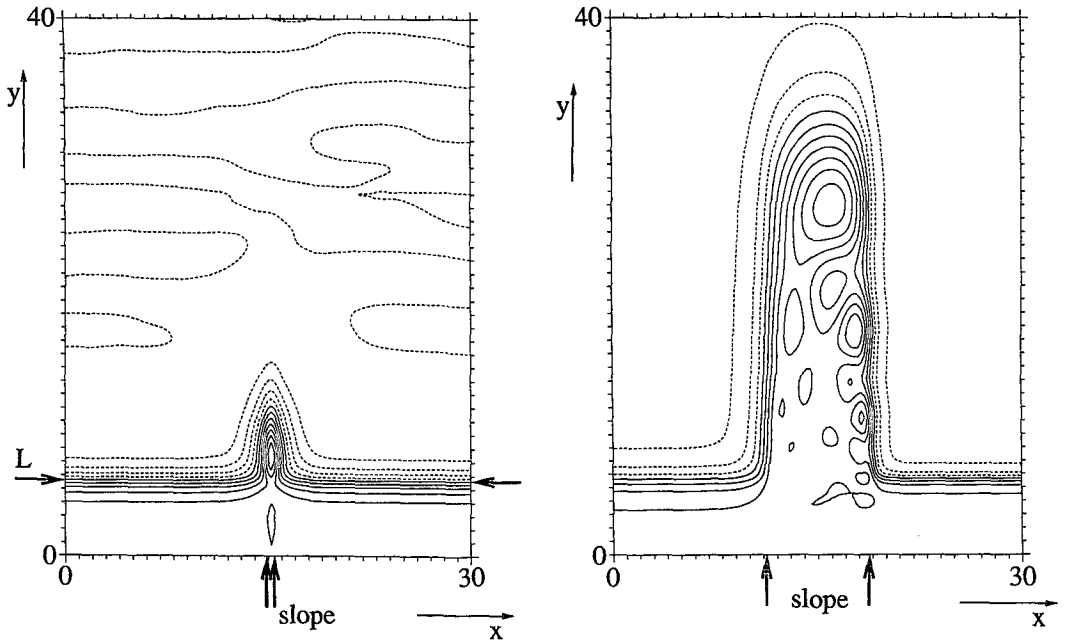

FIG. 9. Plan view of the surface height contours after 50 inertial periods for (a) $W/R = 0.5$ and (b) $W/R = 7.5$. $\sigma = 0.1$. Distance is in units of R_D.

5. Discussion and summary

Rossby adjustment across a slope in a homogeneous fluid generates a tongue along the slope in a manner similar to adjustment over a step. Because the flux in the jet depends on the depth, the flux differential at the slope causes an accumulation or depletion of fluid over the slope. The flow bends around the accumulation/depletion and the process continues, producing a tongue. The tongue width is dependent on the width of the slope and a region of slowly eddying fluid is found in the center of the tongue bounded by jets on both sides. Dispersion effects result in a series of peaks and troughs in the tongue. Unlike the step case these are not symmetric and they are displaced toward the shallow edge of the slope. The finite width slope allows cross escarpment modes and as time progresses, the tongue organizes into trains of waves with the mode-0 waves leading followed by mode 2 and 4. The odd number modes have small amplitudes.

The finite width slope allows wave and energy propagation in both directions along the slope. Total kinetic energy along the slope in the direction the long waves propagate grows without bound as kinetic energy is continually extracted from potential energy. This energy is in the zero-wavenumber double Kelvin wave. Kinetic energy in the other direction was shown to be bounded above by 20% of the energy in all other wavenumbers for the case of a 5 Rossby radii wide slope and a depth change of 50%.

The tongue propagates alongslope with the shallow water on the right in the Northern Hemisphere at a rate given by the long wave speed of the mode-0 double Kelvin wave, which, in turn, depends primarily on the parameter σ, which is dependent on the gradient of the slope. The timescale of the tongue formation is given by $1/\sigma f$ and as a "rule of thumb" for general flow problems, if the background flow is steady over a timescale large compared to $1/\sigma f$, the effect of a slope on the flow should not be neglected. The shape of the tongue depends on the width of the slope, W/R. As W/R increases, the flow becomes more asymmetric with the disturbance propagating faster and the peaks/troughs become closer to the shallow edge of the slope.

The tongue approaches a steady state consisting of stagnant fluid over the slope and jets traveling up along one edge of the slope and down along the other. The presence of the topography enables more potential energy to be released from the initial discontinuity in surface elevation. The concept of a greater amount of energy release due to a more complicated geometry can be generalized by realizing that the major contribution to the change in kinetic energy, when moving from simple to complicated geometry, is the length of the geostrophic jet.[1] In steady geostrophic flow, the flow is

[1] The other possible contribution is due to movement of the jet into deeper water; the kinetic energy is proportional to $h^{1/2}$.

along the depth contours. Thus, any geometry that initially causes the flow to cross depth contours will cause more kinetic energy to be released from the potential energy field.

The finite width slope, as opposed to a step, allows a multitude of modes and, more importantly, allows propagation in both directions along the slope. However, it has been shown that the steady state is similar to that over a step (except for the stagnant region over the slope itself) and the presence of a wall has little effect if the propagation of the long waves is away from the wall.

The effect of a nearby wall perpendicular to the slope (parallel to the slope gradient) on flow over a slope depends on its orientation. If the wall is oriented so that the long double Kelvin waves travel away from the wall, the flow is modified but not greatly changed. An analytical solution for a step abutting a wall is given in Johnson and Davey (1990). Willmott and Grimshaw (1991) considered the related problem of flow over a wedge-shaped escarpment. This particular geometry reduces the effect of the higher-mode double Kelvin waves. The problem of Kelvin waves crossing stepped topography abutting a wall has been considered by Johnson (1990) and over continuous topography including a linear slope by Johnson (1993). Figure 2 from Johnson (1993) shows a low-frequency wave over a linear escarpment; the flow near the wall is similar to the development of the tongue over the slope seen in Fig. 6 here. However, higher cross-slope modes do not seem to form to the same extent in the case of Kelvin wave scattering as they do in the Rossby adjustment problem.

If, on the other hand, the long double Kelvin waves travel into the wall, the jet is squeezed against the wall and accelerates, producing a nonlinear steady state current (Allen 1988).

Generalization of this work to two-layered stratified flow is considered in Allen (1988) and Willmott and Johnson (1995) have considered two-layer flow over a step.

Acknowledgments. I wish to acknowledge the support and encouragement of my doctoral supervisor, Dr. P. F. Linden. The code was based on a code kindly given to me by Dr. M. Davey. M. England prepared one of the diagrams; J. Tam and D. Latornell assisted with the computing. I wish to thank Dr. A. Willmott, Dr. R. E. Thomson, and anonymous referees for their constructive criticism of a previous version of this manuscript. This work was partially supported by an NSERC postgraduate fellowship and by an NSERC operating grant, both to the author.

REFERENCES

Allen, S. E., 1988: Rossby adjustment over a slope. Ph.D. thesis, University of Cambridge, 206 pp.

Gill, A. E., 1982: *Atmosphere–Ocean Dynamics.* Academic Press, 662 pp.

——, M. K. Davey, E. R. Johnson, and P. F. Linden, 1986: Rossby adjustment over a step. *J. Mar. Res.*, **44,** 713–738.

Johnson, E. R., 1985: Topographic waves and the evolution of coastal currents. *J. Fluid Mech.*, **160,** 499–509.

——, 1990: The low-frequency scattering of Kelvin waves by stepped topography. *J. Fluid Mech.*, **215,** 23–44.

——, 1993: The low-frequency scattering of Kelvin waves by continuous topography. *J. Fluid Mech.*, **248,** 173–201.

——, and M. K. Davey, 1990: Free-surface adjustment and topographic waves in coastal currents. *J. Fluid Mech.*, **219,** 273–289.

Longuet-Higgins, M. S., 1968a: On the trapping of waves along a discontinuity of depth in a rotating ocean. *J. Fluid Mech.*, **31,** 417–434.

——, 1968b: Double Kelvin waves with continuous depth profiles. *J. Fluid Mech.*, **34,** 49–80.

Rhines, P. B., 1967: Slow oscillations in an ocean of varying depth. Ph.D. thesis, University of Cambridge.

Spitz, Y. H., and D. Nof, 1991: Separation of boundary currents due to bottom topography. *Deep-Sea Res.*, **38,** p. 1.

Willmott, A. J., 1984: Forced double Kelvin waves in a stratified ocean. *J. Mar. Res.*, **42,** 319–358.

——, and R. H. J. Grimshaw, 1991: The evolution of coastal currents over a wedge-shaped escarpment. *Geophys. Astrophys. Fluid Dyn.*, **57,** 19–48.

——, and E. R. Johnson, 1995: On geostrophic adjustment of a two-layer, uniformly rotating fluid in the presence of a step escarpment. *J. Mar. Res.*, **53,** 49–77.